ELSEVIER

Nuclear Engineering and Design 203 (2001) 117–131

Nuclear Engineering and Design

www.elsevier.com/locate/nucengdes

Flow regime transition criteria for upward two-phase flow in vertical narrow rectangular channels

Takashi Hibiki *, Kaichiro Mishima

Department of Nuclear Energy Science, Research Reactor Institute, Kyoto University, Kumatori-cho, Sennan-gun, Osaka 590-0494, Japan

Received 17 August 1999; received in revised form 1 June 2000; accepted 5 June 2000

Abstract

In relation to the cooling system of high performance microelectronics, a high power research reactor with plate type fuels and plasma facing components of a fusion reactor, study of two-phase flow in a narrow rectangular channel has been paid considerable attention, recently. For the two-fluid model, direct geometrical parameters such as the void fraction should be used in flow-regime criteria. From this point of view, flow-regime transition criteria for vertical upward flows in narrow rectangular channels have been developed considering the mechanisms of flow-regime transitions. The basic concept of the present modeling followed the Mishima and Ishii model for vertical upward two-phase flows in round tubes. Newly developed criteria have been compared with the existing experimental data for air–water flows in narrow rectangular channels with the gaps of 0.3–17 mm. The present criteria showed satisfactory agreements with those data. Further comparisons with data for steam–water in a rectangular channel at relatively high system pressures have been made. The results confirmed that the present flow-regime transition criteria could be applied over wide ranges of parameters as well as to boiling flow.

1. Introduction

In relation to the cooling system of high performance microelectronics, a high power research reactor with plate type fuels and plasma facing components of a fusion reactor, study of two-phase flow in a narrow rectangular channel has been paid considerable attention recently. It is anticipated that the characteristics of two-phase flow in such a narrow channel with a large aspect ratio differ from those in other channel geometries, because of the significant restriction of the bubble shape, which, consequently, may affect the heat removal by boiling under abnormal operating conditions.

In analyzing two-phase flow transients, a two-fluid model is very important because of its detailed description of thermohydraulic transients and phase interactions. The main difficulties in modeling arise from the existence of interfaces between phases and discontinuities associated with them. The internal structures of two-phase flow are classified by the flow regimes or flow patterns. Various transfer mechanisms between

* Corresponding author. Tel.: +81-724-512373; fax: +81-724-512461.

E-mail address: hibiki@rri.kyoto-u.ac.jp (T. Hibiki).

0029-5493/01/$ - see front matter
PII: S0029-5493(00)00306-X

two-phase mixture and the wall, as well as between two phases, depend on the flow regimes. This leads to the use of regime dependent correlations together with two-phase flow-regime criteria. From this point of view, many works on the flow regime have been undertaken even in small channels. Wilmarth and Ishii (1994, 1997) extensively reviewed the studies, which were performed on two-phase flow in rectangular channels with gap width smaller than 7 mm by 1991. Recent studies on flow regime in narrow rectangular channels can be also summarized as follows.

Moriyama et al. (1992a,b) measured flow pattern, pressure drop, void fraction and phase velocity for N_2-R113 adiabatic gas–liquid two-phase flow in narrow channels with the gaps of 5–100 μm between horizontal parallel plates and flow pattern, pressure drop and heat transfer for R113 boiling two-phase flow in narrow channels with the gaps of 35–110 μm between horizontal parallel plates. Mishima et al. (1993) performed measurements of flow regime, void fraction, slug bubble velocity, and pressure loss for rectangular channels with the gaps of 1.0, 2.4, and 5.0 mm. They discussed the effect of the channel gap on the flow characteristics extensively. Wilmarth and Ishii (1994, 1997) measured flow regime, void fraction and interfacial area concentration of adiabatic concurrent vertical and horizontal air–water flow in narrow rectangular channels with the gaps of 1 and 2 mm. They compared their flow regime maps with the existing ones as well as the models of flow regime transition criteria basically developed for a round pipe. Bonjour and Lallemand (1998) carried out an experimental study to identify the different regimes of natural convective boiling of R113 in a narrow rectangular vertical channel with the gap size ranging from 0.5 to 2 mm. They observed three boiling regimes, such as nucleate boiling with isolated deformed bubbles, nucleate boiling with coalesced bubbles, and partial dry out and developed a new flow pattern map for confined boiling based on the Bond number and a reduced heat flux (ratio of the heat flux to the critical heat flux). Xu (1999) conducted experimental investigations for adiabatic air–water two-phase flow in vertical rectangular channels with the gaps of 0.3, 0.6 and 1.0 mm. They reported that observed flow regimes (bubbly, slug, churn, and annular flow) in channels with the gaps of 0.6 and 1.0 mm were similar to those found in the previous studies and that observed flow regimes (cap-bubbly, slug-droplet, churn and annular-droplet flow) in the channel with the gap of 0.3 mm were different from the previous studies.

Although, some studies have been performed on the observation of flow regimes in a narrow rectangular channel, very little amount is available for the modeling of flow regime transition criteria for two-phase flow in a narrow rectangular channel. Recently, Xu et al. (1999) proposed a preliminary model for flow regime transition criteria of two-phase flow in a rectangular channel and applied the model to predicting flow regime transition boundaries of adiabatic air–water flow in narrow rectangular channels. However, it turned out that the model could not predict the flow regime transition boundaries in narrow rectangular channels satisfactorily and they concluded that a new model should need to be developed.

In view of this, new flow-regime transition criteria for upward gas–liquid flow in vertical narrow rectangular channels have been developed in this study. Four basic flow regimes such as bubbly flow, slug flow, churn flow, and annular flow, have been analyzed. Newly developed criteria have been compared with the existing experimental data for air–water flows in narrow rectangular channels with the gaps of 0.3–17 mm as well as for steam–water flows in a rectangular channel with the gap of 3.175 mm at relatively high system pressures.

2. Criteria for flow-regime transitions

2.1. Bubbly flow to slug flow transition

It is widely recognized that the bubbly flow to slug flow transition in a round tube occurs at the void fraction approximately 0.3. Mishima and Ishii (1984) derived this criterion based on a very simple geometrical consideration only. The void fraction at bubbly-to-slug flow transition in a narrow rectangular channel can be obtained in the

similar way. The difference is that the narrow gap allows of only two-dimensional bubble fluctuation. Suppose bubbles distribute themselves in a square lattice pattern in which each bubble fluctuates as shown in Fig. 1. It is assumed that there is a sphere of influence around each bubble. The possibility of collisions and coalescences is considered to increase significantly if the maximum possible distance l between two bubbles becomes less than a projected diameter of a flat bubble $2R_b$ as shown in Fig. 1. The bubbly flow to slug flow transition is considered to occur under this condition, namely

$$\alpha = \frac{\pi R_b^2}{16 R_b^2} = 0.196 \cong 0.2 \tag{1}$$

The relationship between j_g and j_f at the transition is given by the drift flux correlation for bubbly flow (Ishii, 1977) as

$$j_f = \left(\frac{1}{\alpha C_0} - 1\right) j_g - \frac{V_{gj}}{C_0}$$

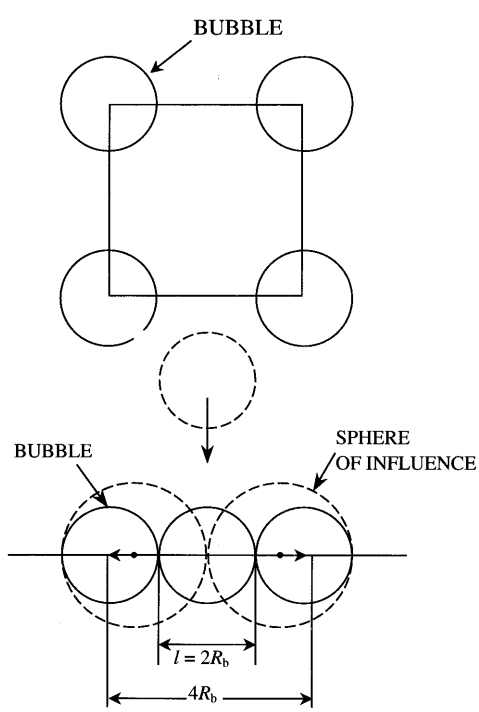

Fig. 1. Bubble packing and coalescence pattern.

where $C_0 = 1.35 - 0.35\sqrt{\frac{\rho_g}{\rho_f}}$ and

$$V_{gj} = \sqrt{2}\left(\frac{\sigma g \Delta\rho}{\rho_f^2}\right)^{1/4} (1-\alpha)^{1.75} \tag{2}$$

It should be noted that the void fraction at the transition varies from 0.2 to 0.3 with increasing the channel gap. Here, the dependence of void fraction on the channel gap s may be roughly expressed by

$$\alpha = 0.2 \text{ for } s < D_b,$$

$$\alpha = \frac{s}{20 D_b} + 0.15 \text{ for } D_b \le s \le 3D_b,$$

$$\alpha = 0.3 \text{ for } s > 3D_b \tag{3}$$

where, D_b denotes the equivalent diameter of a sphere. It should be also noted here that the drift velocity V_{gj} becomes 0 for a narrow gap. This was observed for a round tube with an inner diameter smaller than 5 mm (Mishima and Hibiki, 1996). Mishima et al. (1993), Wilmarth and Ishii (1997) also pointed out that the drift velocity was almost 0 for the gap smaller than 2.4 and 2 mm corresponding to the equivalent channel diameter ($D_h = 2ws/(w+s)$; w, channel width) of 4.5 and 3.5 mm, respectively.

2.2. Slug flow to churn flow transition

The slug flow to churn flow transition is assumed to occur when the mean void fraction over the entire region exceeds that over the slug–bubble section (Mishima and Ishii, 1984). They derived the local void fraction $\alpha(h)$ at the distance h from the nose and the mean void fraction α_m over the slug–bubble section at the transition as follows:

$$\alpha(h) = \frac{\sqrt{2gh\Delta\rho/\rho_f}}{\sqrt{2gh\Delta\rho/\rho_f} + (C_0 - 1)j + V_{gj}} \tag{4}$$

$$\alpha_m = 1 - 0.813 X^{0.75}$$

$$\text{where } X \equiv \sqrt{\frac{\rho_f}{2g\Delta\rho L_b}}[(C_0 - 1)j + V_{gj}],$$

$$C_0 = 1.35 - 0.35\sqrt{\frac{\rho_g}{\rho_f}}, \tag{5}$$

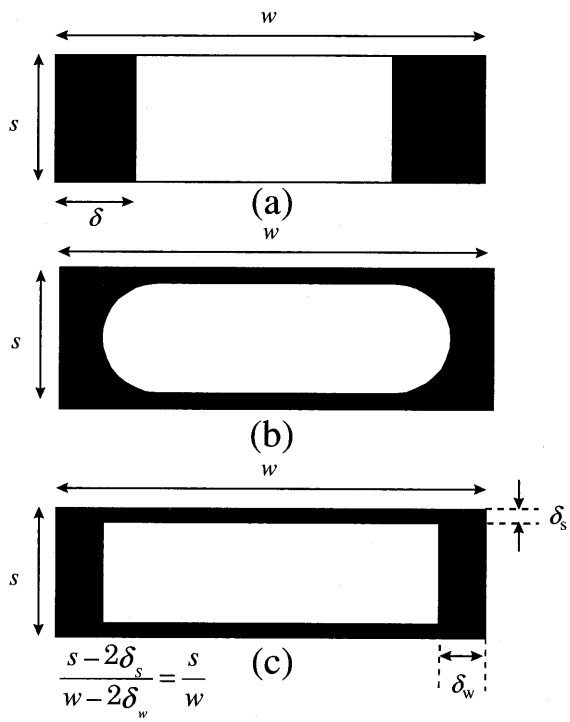

Fig. 2. Film models in a narrow rectangular channel.

and

$$V_{gj}=\left(0.23+0.13\frac{s}{w}\right)\sqrt{\frac{\Delta\rho g w}{\rho_f}}. \tag{6}$$

The drift velocity for slug bubbles in a rectangular channel obtained by Griffith (1963), Eq. (6) is used here. The mean slug–bubble length L_b at the transition from the slug-to-churn flow regime can be estimated by applying the basic concept of Mishima and Ishii (1984) model to the two-phase flow in the narrow rectangular channel. Namely, somewhere below the nose of a slug bubble, the gravity force on the liquid film is completely balanced by the wall shear stress and the flow becomes fully developed. At a section below this point, there exists a small adverse pressure gradient for the downward liquid film flow. Since the liquids are no longer accelerating in the downward direction, the liquid film becomes unstable due to flow separation and film instability. Thus, beyond the terminal velocity point of a film, interface disturbances will lead to a cut-off of the slug bubble. Based upon the observations (Mishima et al., 1993) and the measurement of the conductivity film thickness probe (Wilmarth and Ishii, 1997), it is assumed that the liquid flowing down the wide side walls can be neglected when compared with that on the narrower side walls (see Fig. 2a). This assumption is valid for the rectangular channel with the gap smaller than about 2.4 mm. Then, the force balance on the liquid film around the slug bubble in a narrow rectangular channel gives

$$f\frac{1}{2}\rho_f v_{fsb}^2(2\delta+s)=\Delta\rho g\delta s,\quad \alpha_{sb}=1-\frac{2\delta}{w}. \tag{7}$$

The wall friction factor f is assumed to be in the form

$$f=C_f\left[\frac{(1-\alpha_{sb})v_{fsb}D_h}{\nu_f}\right]^{-m}$$
$$m=1 \text{ for laminar flow,} \tag{8}$$
$$m=0.25 \text{ for turbulent flow.}$$

The shape factor $C_{f,l}$ for a laminar flow in the rectangular channel is given by (Itatani, 1966).

$$C_{f,l}=\frac{128w^2}{(w+s)^2\chi},$$
$$\chi=2.25241+5.94208\xi-4.59384\xi^2+1.60646\xi^3-0.2071\xi^4,\qquad \xi\equiv\log\left(\frac{w}{s}\right). \tag{9}$$

The shape factor $C_{f,t}$ for a turbulent flow is given by (Sadatomi et al., 1982)

$$\frac{C_{f,t}}{C_{f,t0}}=\left(0.0154\frac{C_{f,l}}{C_{f,l0}}-0.012\right)^{1/3}+0.85, \tag{10}$$

where, $C_{f,l0}(=16)$ and $C_{f,t0}(=0.079)$ denote the shape factor of a round tube for laminar and turbulent flows, respectively. The terminal film velocity v_{fsb} in the slug–bubble section is derived from Eqs. (7) and (8), thus

$$v_{fsb}=(1-\alpha_{sb})^{\left(\frac{m}{2-m}\right)}\left[\left(\frac{D_h}{\nu_f}\right)^{-m}\frac{C_f\rho_f}{\Delta\rho g s}\right]^{\left(\frac{1}{m-2}\right)}. \tag{11}$$

The void fraction α_{sb} corresponding to the terminal film velocity can be deduced from Eqs. (11) and (12), then

$$v_{\mathrm{fsb}} = \frac{\alpha_{\mathrm{sb}} v_{\mathrm{gs}} - j}{1 - \alpha_{\mathrm{sb}}}. \tag{12}$$

The resulting equation is

$$\alpha_{\mathrm{sb}} = \frac{j + (1-\alpha_{\mathrm{sb}})^{\left(\frac{2}{2-m}\right)} [(D_{\mathrm{h}}/v_{\mathrm{f}})^{-m} (C_{\mathrm{f}}\rho_{\mathrm{f}}/\Delta\rho g s)]^{\left(\frac{1}{m-2}\right)}}{C_0\, j + V_{\mathrm{gj}}} \tag{13}$$

The above equation can be solved by applying the approximation of $(1-\alpha_{\mathrm{sb}})^{\left(\frac{2}{2-m}\right)} \cong \gamma(1-\alpha_{\mathrm{sb}})$ ($\gamma = 0.15$ and 0.7 for laminar and turbulent flows, respectively) to Eq. (13) as

$$\alpha_{\mathrm{sb}} = \frac{j + \gamma\{(D_{\mathrm{h}}/v_{\mathrm{f}})^{-m} C_{\mathrm{f}}\rho_{\mathrm{f}}/(\Delta\rho g s)\}^{\left(\frac{1}{m-2}\right)}}{C_0\, j + V_{\mathrm{gj}} + \gamma\{(D_{\mathrm{h}}/v_{\mathrm{f}})^{-m} C_{\mathrm{f}}\rho_{\mathrm{f}}/(\Delta\rho g s)\}^{\left(\frac{1}{m-2}\right)}}$$

$$= \frac{j + \gamma\{(D_{\mathrm{h}}/v_{\mathrm{f}})^{-m} C_{\mathrm{f}}\rho_{\mathrm{f}}/(\Delta\rho g s)\}^{\left(\frac{1}{m-2}\right)}}{[j + \gamma\{(D_{\mathrm{h}}/v_{\mathrm{f}})^{-m} C_{\mathrm{f}}\rho_{\mathrm{f}}/(\Delta\rho g s)\}^{\left(\frac{1}{m-2}\right)}] + (C_0 - 1)j + V_{\mathrm{gj}}}. \tag{14}$$

Finally, the mean slug–bubble length at the transition from the slug-to-churn flow regime is obtained by comparing Eq. (14) with Eq. (4) and letting $h = L_{\mathrm{b}}$ as

$$L_{\mathrm{b}} = \frac{\rho_{\mathrm{f}}}{2\Delta\rho g}\left[j + \left\{ \left(\frac{D_{\mathrm{h}}}{v_{\mathrm{f}}}\right)^{-m} \frac{C_{\mathrm{f}}\rho_{\mathrm{f}}}{\Delta\rho g s} \right\}^{\left(\frac{1}{m-2}\right)} \gamma \right]^2. \tag{15}$$

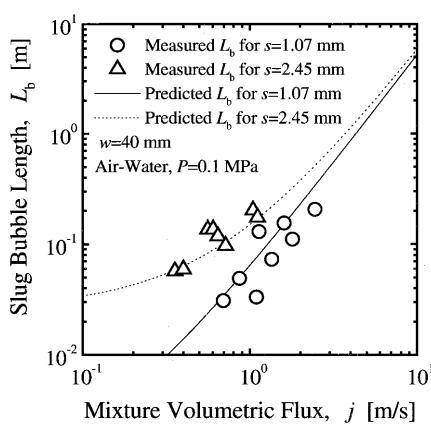

Fig. 3. Comparison of mean slug bubble length with the experimental data by Mishima et al. (1993).

Fig. 3 shows a reasonable agreement between measured slug–bubble lengths (Mishima et al., 1993) and ones predicted by Eq. (15) with $m = 1$ and $\gamma = 0.15$ for the laminar flow. From Eqs. (5) and (15), the transition criterion becomes

$$\alpha \geq 1 - 0.813 X^{0.75}$$

$$\text{where } X = \frac{(C_0 - 1)j + V_{\mathrm{gj}}}{j + \gamma\{(D_{\mathrm{h}}/v_{\mathrm{f}})^{-m} C_{\mathrm{f}}\rho_{\mathrm{f}}/(\Delta\rho g s)\}^{\left(\frac{1}{m-2}\right)}}$$

$$(s \leq 2.4 \text{ mm}). \tag{16}$$

By using Eq. (16) and the drift-flux model, the slug-to-churn flow transition criterion can be presented in terms of j_{g} and j_{f} under steady-state fully developed flow conditions.

On the other hand, for a rectangular channel with the gap larger than 2.4 mm, the liquid flows down not only the narrower side walls but also the wide side walls (see Fig. 2b). This requires the following force balance on the liquid film around the slug bubble instead of Eq. (7).

$$f\frac{1}{2}\rho_{\mathrm{f}} v_{\mathrm{fsb}}^2 \times 2(w+s) = \Delta\rho g w s (1 - \alpha_{\mathrm{sb}}). \tag{17}$$

The following equation can be derived in the similar manner to Eq. (16).

$$\alpha \geq 1 - 0.813 X'^{0.75} \quad \text{where}$$

$$X' = \frac{(C_0 - 1)j + V_{\mathrm{gj}}}{j + \gamma'\{(D_{\mathrm{h}}/v_{\mathrm{f}})^{-m} C_{\mathrm{f}}\rho_{\mathrm{f}}(w+s)/(\Delta\rho g w s)\}^{\left(\frac{1}{m-2}\right)}}$$

$$(s > 2.4 \text{ mm}), \tag{18}$$

where, $\gamma' = 0.02$ or 0.25 in the approximation of $(1-\alpha_{\mathrm{sb}})^{3/(2-m)} \cong \gamma'(1-\alpha_{\mathrm{sb}})$ for the laminar or turbulent flow, respectively.

2.3. Churn flow to annular flow transition

The churn-to-annular flow transition criterion has been developed previously (Ishii, 1977), assuming two different mechanisms, (a) flow reversal in

the liquid film section along large bubbles; (b) destruction of liquid slugs or large waves by entrainment or deformation. It is assumed here that the same mechanisms work for a narrow rectangular channel, too.

Flow reversal condition can be derived as follows. The relationship among the pressure drop, gravity force and the shear stresses in the liquid film is expressed as (see Fig. 2c),

$$-\frac{\mathrm{d}p}{\mathrm{d}z}=\rho_{\mathrm{f}}g-\frac{2(s+w)\sqrt{\alpha}}{ws(1-\alpha)}\tau_{\mathrm{i}}+\frac{2(s+w)}{ws(1-\alpha)}\tau_{\mathrm{wf}} \tag{19}$$

As for the gas core, we have

$$-\frac{\mathrm{d}p}{\mathrm{d}z}=\rho_{\mathrm{g}}g+\frac{2(s+w)\sqrt{\alpha}}{ws\alpha}\tau_{\mathrm{i}}, \tag{20}$$

where, the Greek symbols τ_{i} and τ_{wf} denote the interfacial shear stress, and the wall shear stress in the liquid film, respectively. It should be noted here that the wetted perimeter of the gas–liquid interface is given by $2(s+w)\sqrt{\alpha}$. Eliminating the pressure drop term from Eqs. (19) and (20), the following equation is obtained

$$\Delta\rho g=\frac{2(s+w)\sqrt{\alpha}}{ws\alpha(1-\alpha)}\tau_{\mathrm{i}}-\frac{2(s+w)}{ws(1-\alpha)}\tau_{\mathrm{wf}}. \tag{21}$$

Here, the following equations for the interfacial shear stress and the wall stress in the liquid film are assumed:

$$\tau_{\mathrm{i}}=\frac{f_{\mathrm{i}}}{2}\rho_{\mathrm{g}}v_{\mathrm{r}}^2, \tag{22}$$

$$\tau_{\mathrm{wf}}=\frac{f_{\mathrm{f}}}{2}\rho_{\mathrm{f}}v_{\mathrm{f}}|v_{\mathrm{f}}|, \tag{23}$$

where, v_{r} is the relative velocity between two phases. Substituting Eqs. (22) and (23) into Eq. (21), the following relation is derived.

$$\frac{f_{\mathrm{i}}\rho_{\mathrm{g}}(s+w)\sqrt{\alpha}}{\Delta\rho gws\alpha}\left(\frac{j_{\mathrm{g}}}{\alpha}-\frac{j_{\mathrm{f}}}{1-\alpha}\right)^2-\frac{f_{\mathrm{f}}\rho_{\mathrm{f}}(s+w)j_{\mathrm{f}}|j_{\mathrm{f}}|}{\Delta\rho gws(1-\alpha)^2}=1-\alpha. \tag{24}$$

For flow reversal condition, letting $j_{\mathrm{f}}=0$, the resulting equation is

$$j_{\mathrm{g}}=\sqrt{\frac{\Delta\rho g}{\rho_{\mathrm{g}}}\alpha^3(1-\alpha)\left\{\frac{f_{\mathrm{i}}(s+w)\sqrt{\alpha}}{ws}\right\}^{-1}}. \tag{25}$$

Here, the following equation for the interfacial friction factor is assumed (Wallis, 1969):

$$f_{\mathrm{i}}=0.005[1+75(1-\alpha)]. \tag{26}$$

Finally, the churn-to-annular transition criterion is deduced as

$$j_{\mathrm{g}}=\sqrt{\frac{\Delta\rho g}{\rho_{\mathrm{g}}}\alpha^3(1-\alpha)\left[\frac{0.005\{1+75(1-\alpha)\}(s+w)\sqrt{\alpha}}{ws}\right]^{-1}}. \tag{27}$$

However, in the range of α relevant to the present case, the churn-to-annular flow transition criterion can be approximated by

$$j_{\mathrm{g}}=\sqrt{\frac{3\Delta\rho gD_{\mathrm{h}}}{2\rho_{\mathrm{g}}}}(\alpha-0.11), \tag{28}$$

where, α should satisfy the condition given by Eq. (16) or Eq. (18). The transition criterion in the j_{g}–j_{f} plane is obtained from Eq. (28) and the following drift flux correlation for churn flow (Ishii, 1977):

$$v_{\mathrm{g}}=C_0\,j+V_{\mathrm{gj}},\qquad C_0=1.35-0.35\sqrt{\frac{\rho_{\mathrm{g}}}{\rho_{\mathrm{f}}}},$$
$$V_{\mathrm{gj}}=\sqrt{2}\left(\frac{\sigma g\Delta\rho}{\rho_{\mathrm{f}}^2}\right)^{1/4}. \tag{29}$$

On the other hand, the second criterion can be obtained from the onset of droplet entrainment. The onset of entrainment criteria for film flow has been developed from a force balance on the liquid wave crest between the shearing force of the vapor drag and the retaining force of the surface tension (Ishii, 1977). Since this criterion may be determined by the local condition of the liquid film, the channel geometry may not affect the model significantly. In this study, the model of Ishii (1977) is used for the prediction of the churn-to-annular and slug-to-annular flow boundaries. This entrainment induced flow transition is given by

$$j_{\mathrm{g}}\geq\left(\frac{\sigma g\Delta\rho}{\rho_{\mathrm{g}}^2}\right)^{1/4}N_{\mu\mathrm{f}}^{-0.2},\quad N_{\mu\mathrm{f}}\equiv\frac{\mu_{\mathrm{f}}}{[\rho_{\mathrm{f}}\sigma\sqrt{\sigma/(g\Delta\rho)}]^{1/2}}. \tag{30}$$

The second criterion is applicable to a flow in a large gap channel given by

Table 1
Newly developed flow regime transition criteria for a rectangular channel

Flow regime transitions	Modeled mechanisms	Flow regime transition criteria
Bubbly-to-slug	The transition is postulated to occur due to significant increase in the possibility of bubble collisions and coalescence when the bubble distance becomes less than a projected diameter of a flat bubble.	$\alpha=0.2$ for $s<D_b$, $\alpha=\frac{s}{20D_b}+0.15$ for $D_b\le s\le 3D_b$, $\alpha=0.3$ for $s>3D_b$
Slug-to-churn	The transition is postulated to occur when the mean void fraction over the entire region exceeds that over the slug–bubble section.	(a) $s\le 2.4$ mm $\alpha\ge 1-0.813X^{0.75}$, $X=\frac{(C_0-1)j+V_{gj}}{j+\gamma\{(D_h/\nu_f)^{-m}C_f\rho_f/(\Delta\rho gs)\}^{\left(\frac{1}{m-2}\right)}}$, (b) $s>2.4$ mm $\alpha\ge 1-0.813X'^{0.75}$, $X'=\frac{(C_0-1)j+V_{gj}}{j+\gamma'\{(D_h/\nu_f)^{-m}C_f\rho_f(w+s)/\Delta(\rho gws)\}^{\left(\frac{1}{m-2}\right)}}$
Churn-to-annular	The transition is postulated to occur due to (a) flow reversal in the liquid film section along large bubbles or (b) destruction of liquid slugs or large waves by entrainment or deformation.	(a) flow reversal $j_g=\sqrt{\frac{3\Delta\rho gD_h}{2\rho_g}}(\alpha-0.11)$, (b) destruction of liquid slugs or large waves by entrainment or deformation $j_g\ge\left(\frac{\sigma g\Delta\rho}{\rho_g^2}\right)^{1/4}N_{\mu f}^{-0.2}$, $N_{\mu f}\equiv\frac{\mu_f}{[\rho_f\sigma\sqrt{\sigma/(g\Delta\rho)}]^{1/2}}$ for $D_h>\frac{2\sqrt{\sigma/(\Delta\rho g)}N_{\mu f}^{-0.4}}{3\{(1-0.11C_0)/C_0\}}$
Slug-to-churn	The transition is postulated to occur due to destruction of liquid slugs or large waves by entrainment or deformation.	$j_g\ge\left(\frac{\sigma g\Delta\rho}{\rho_g^2}\right)^{1/4}N_{\mu f}^{-0.2}$, $N_{\mu f}\equiv\frac{\mu_f}{[\rho_f\sigma\sqrt{\sigma/(g\Delta\rho)}]^{1/2}}$

$$D_h>\frac{2\sqrt{\sigma/(\Delta\rho g)}N_{\mu f}^{-0.4}}{3\{(1-0.11C_0)/C_0\}}, \tag{31}$$

Therefore, the second criterion from the onset of entrainment is applicable to predict the occurrence of the annular-mist flow or to predict the churn-to-annular flow transition in a large channel.

2.4. Flow regime map

A flow-regime map can be drawn by using newly developed transition criteria summarized in Table 1. Fig. 4 shows an example of a flow-regime map for air–water flow in a rectangular channel with the gap of 1.0 mm and the width of 40 mm at the atmospheric pressure. The conditions in

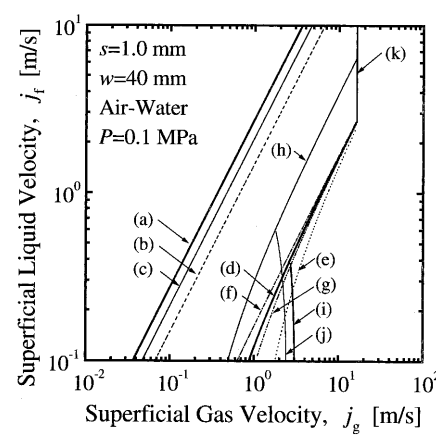

Fig. 4. Flow regime map based on newly developed transition criteria.

Table 2
Conditions in calculation of flow regime transition criteria

Index	Flow regime transition	Equation used in calculation	Distribution parameter	Friction factor
(a)	Bubbly–slug	Eq. (2), $\alpha = 0.2$, $V_{gj} = 0$	$1.35 - 0.35(\rho_g/\rho_f)^{0.5}$	Not necessary
(b)	Bubbly–slug	Eq. (2), $\alpha = 0.3$, $V_{gj} = 0$	$1.35 - 0.35(\rho_g/\rho_f)^{0.5}$	Not necessary
(c)	Bubbly–slug	Eq. (2), $\alpha = 0.2$, $V_{gj} = 0$	1.6	Not necessary
(d)	Slug–churn	Eq. (16), $V_{gj} = 0$	$1.35 - 0.35(\rho_g/\rho_f)^{0.5}$	Laminar
(e)	Slug–churn	Eq. (16), $V_{gj} = 0$	$1.35 - 0.35(\rho_g/\rho_f)^{0.5}$	Turbulent
(f)	Slug–churn	Eq. (18), $V_{gj} = 0$	$1.35 - 0.35(\rho_g/\rho_f)^{0.5}$	Laminar
(g)	Slug–churn	Eq. (18), $V_{gj} = 0$	$1.35 - 0.35(\rho_g/\rho_f)^{0.5}$	Turbulent
(h)	Slug–churn	Eq. (16), $V_{gj} = 0$	1.6	Laminar
(i)	Churn–annular	Eq. (27), $V_{gj} = 0$	$1.35 - 0.35(\rho_g/\rho_f)^{0.5}$	Not necessary
(j)	Churn–annular	Eq. (27), $V_{gj} = 0$	1.6	Not necessary
(k)	Slug–annular	Eq. (30), $V_{gj} = 0$	$1.35 - 0.35(\rho_g/\rho_f)^{0.5}$	Not necessary

Table 3
Previous works in two-phase flow in narrow rectangular ducts and symbols used in the figures

Investigators	Gap and width (mm)	Length (m)	Working fluids
Hosler (1968)	3.175×25.4	0.610	Steam/water
Sadatomi et al. (1982)	7×20.6; 7, 10, 17×50	3.5, 3.5, 4.1, 4.7	Air/water
Lowry and Kawaji (1988)	0.5, 1.0, 2.0×80	0.080	Air/water
Ali et al. (1993)	0.1465×80	0.240	Air/water
Mishima et al. (1993)	1.0, 2.4, 5.0×40	2.00	Air/water
Wilmarth and Ishii (1994)	1.0×20; 2.0×15	0.630	Air/water
Xu (1999)	0.3, 0.6, 1.0×12	0.260	Air/water

●: Bubbly, ○: B-S, ▲: Slug, △: S-C, ■: Churn, □: C-A, ◆: Annular, ◇: S-A

calculation of flow regime transition criteria are tabulated in Table 2. As discussed later, it is anticipated that the distribution parameter C_0 may vary with decreasing the gap. The effect of the distribution parameter on the flow regime transition criteria is also shown in Fig. 4. The bubbly-to-slug flow transition shifts to the right with increasing the void fraction at the transition ((a)→(b)) and the distribution parameter ((a)→(c)). The slug-to-churn flow transitions shift to the right as the flow structure changes from laminar to turbulent flows ((d)→(e) and (f)→(g)), whereas the slug-to-churn flow and the churn-to-annular flow transitions shift to the left with increasing the distribution parameter ((d)→(h) and (i)→(j)). The predicted slug-to-churn boundaries are independent of flow structure (laminar flow or turbulent flow) for high superficial liquid velocity (see (d), (e), (f) and (g)). Therefore, the equations for laminar flow are used in the prediction of flow regime transition criteria in the next section. The slug-to-annular flow transition boundaries predicted by Eq. (18) for a wider gap test section are located at the left side in comparison to those by Eq. (16) for a narrow gap test section ((d)→(f)). As can be seen from Eq. (30), the distribution parameter does not affect the slug-to-annular flow transition (see (k)).

3. Comparison to existing data

This section discusses the comparison between newly developed flow-regime transition criteria

and existing data for air–water flow and steam–water flow in rectangular channels (see Table 3). In most cases, there are some discrepancies among the flow regime transition boundaries measured by different researchers due to the different methods of observations and definitions of the flow regimes. Moreover, the transition phenomena themselves develop gradually and are affected by upstream conditions such as initial bubble diameter and distribution. Therefore, the transition boundaries should be understood as a band with a certain width proportional to the uncertainty in determining the transition boundaries.

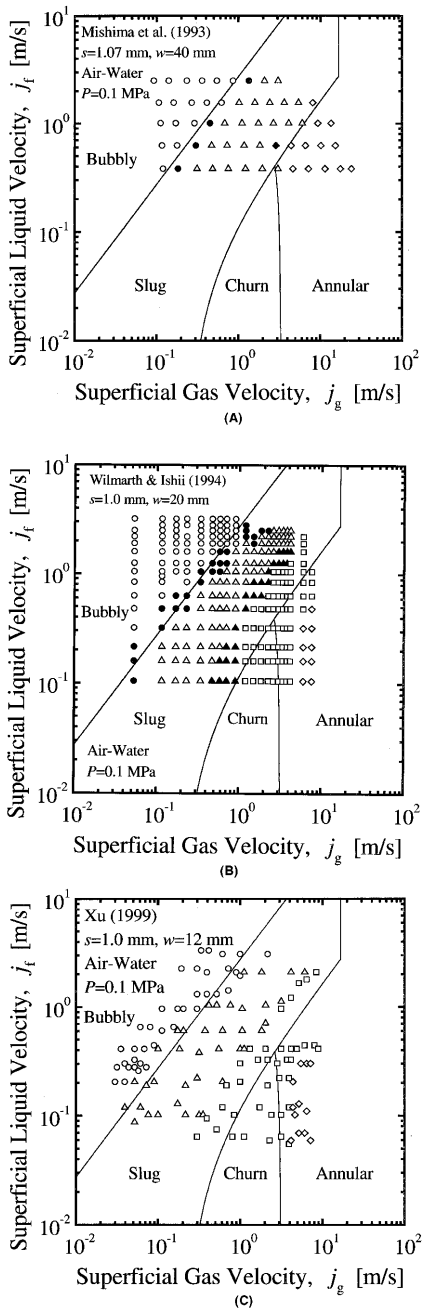

Fig. 5. Flow regime map for 1 mm-gap vertical flow compared with the existing data. (a) Mishima et al. (1993), (b) Wilmarth and Ishii (1994), (c) Xu (1999).

3.1. Air–water flow at atmospheric pressure

Wilmarth and Ishii (1994) compared their data with existing data. The brief summary of their discussion is as follows. As to the comparison of their vertical 1 mm gap test section data with data from Ali et al. (1993), the transition boundaries were similar for bubbly and annular flow regimes; however, somewhat different for slug and churn flow regimes. Wilmarth and Ishii (1994) explained this by the difference in flow geometry since the widths were a factor of four different. The 1 mm gap test section used by Mishima et al. (1993) was only a factor of two different for the width of the test section used by Wilmarth and Ishii, and the data agreed well for the bubbly-to-slug transition. A significant difference was found in the slug-to-churn flow transition boundary. As the comparison of the vertical 2 mm gap test section (Wilmarth and Ishii, 1994) with data from Lowry and Kawaji (1988), the slug-to-churn turbulent transition agreed well except some discrepancy in the bubbly-to-slug transition. The data of Wilmarth and Ishii (1994) agreed very well with the data of Mishima et al. (1993) for all regime transitions except some difference in the annular flow transition. Wilmarth and Ishii also compared existing data with flow regime transition criteria in vertical tubes developed by Mishima and Ishii (1984) and Taitel et al. (1980). The results were less satisfactory.

Here, comparisons were made between the existing experimental data and the newly developed flow-regime transition criteria. Figs. 5 and 6 show the comparisons of the model with experimental

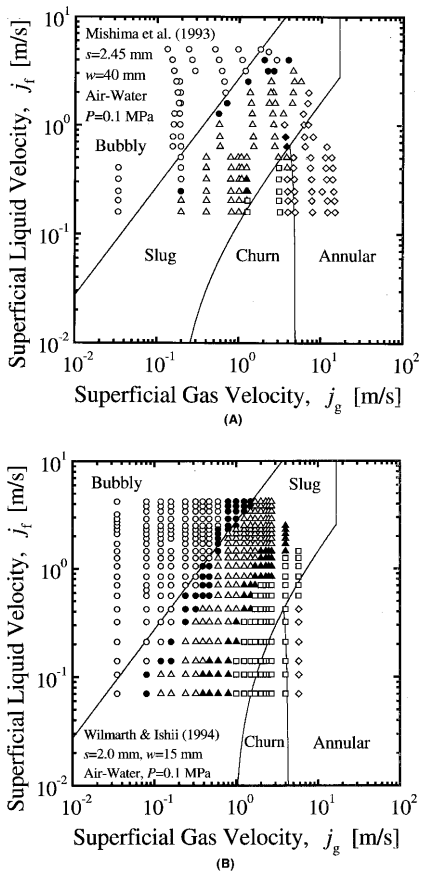

Fig. 6. Flow regime map for 2 mm-gap vertical flow compared with the existing data. (a) Mishima et al. (1993), (b) Wilmarth and Ishii (1994), (c) Xu (1999).

data for the 1 and 2 mm gap test sections, respectively. The drift velocity was set at 0 in calculation and Eq. (16) with the friction factor for the laminar flow was used for the prediction of the slug-to-churn flow transition. Both of 1 and 2 mm gap data agreed well with the predictions for the bubbly-to-slug transition. As can be seen in the figures, the predicted line for the transition to annular flow (slug-to-annular and churn-to-annular) falls reasonably within the band of the annular flow transition region. For the slug-to-churn transition, reasonable agreement between the prediction and the data of Mishima et al. (1993) was obtained for either of the test sections ($s = 1.0$ and 2.4 mm), whereas the results for the data of Wilmarth and Ishii (1994) and Xu (1999) were less satisfactory. It should be noted here that there were some discrepancy between the data of Mishima et al. (1993) and Wilmarth and Ishii (1994) for the slug-to-churn flow transition. As afore-mentioned, this may be due to the different methods of observations, definitions of the flow regimes and different length of the test section. As discussed by Wilmarth and Ishii (1994), the distribution parameter C_0 may affect the boundary of slug-to-churn flow regime transition. Mishima et al. (1993) pointed out that the distribution parameter tended to increase with decreasing channel gap of a rectangular channel. This was also found for a small diameter tube (Mishima and Hibiki, 1996). The increase of the distribution parameter with decreasing gap would cause the

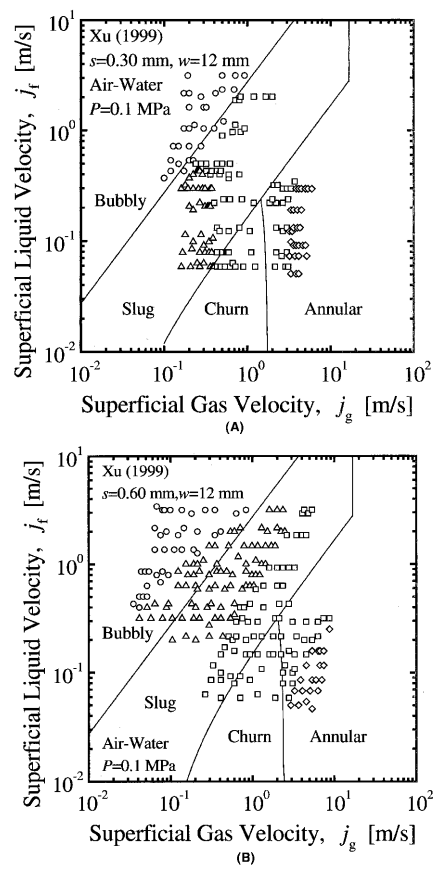

Fig. 7. Flow regime map for 0.3 and 0.6 mm-gap vertical flow compared with the data of Xu (1999). (a) 0.3 mm gap, (b) 0.6 mm gap.

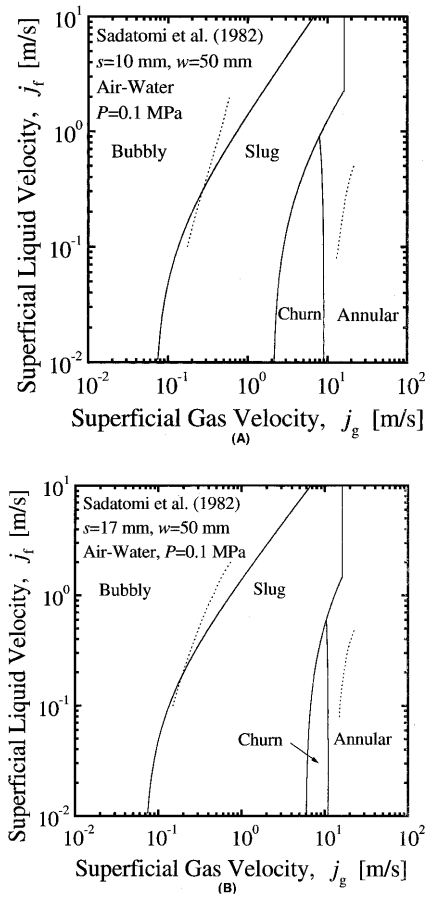

Fig. 8. Flow regime map for 10 and 17 mm-gap vertical flow compared with the data of Sadatomi et al. (1982). (a) 10 mm gap, (b) 17 mm gap.

predicted transition boundaries to shift to the left in the figures (see Fig. 4), which would better agree with experimental data. A new model is needed for the prediction of the distribution parameter for narrow rectangular channels.

Fig. 7 also shows further comparisons of the model with the existing data for smaller gap test sections with the gaps of 0.3 and 0.6 mm. The result similar to the data for 1 and 2 mm gap test sections were also obtained for 0.6-mm gap test section. On the other hand, Xu (1999) reported that the flow regimes in a rectangular channel with the gap of 0.3 mm were different from the classical flow regimes found in medium size channels. They identified three new flow regimes beside the normal churn flow: cap-bubbly, slug-droplet, and annular-droplet flow. In Fig. 7a, open circles, triangles, squares, and diamonds indicate cap-bubbly, slug-droplet, churn, and annular-droplet flows, respectively. The churn flow covers a wide range of liquid flow rates at medium superficial gas velocities. The newly developed model could predict the flow regime transition boundaries satisfactorily except for the newly observed bubbly-to-churn flow transition boundary as well as slug-to-churn flow transition boundary at superficial liquid velocity higher than 0.1 m s^{-1}. Since very little data is available for a rectangular channel with the gap smaller than 1.0 mm, further experimental research should be encouraged for such an extremely narrow channel. A model for the flow regime transition criteria will be modified in accordance with new flow regimes to be observed in a rectangular channel with a micro gap.

In what follows, the applicability of the present model to wider gap channels is examined. Fig. 8 shows the comparisons of the model with experimental data for the 10 and 17 mm gap test section (Sadatomi et al., 1982). Eqs. (2), (6) and (29) were used for drift velocity calculation and Eq. (18) was used as the criterion for the slug-to-churn flow transition. The void fraction at the bubbly-to-slug transition was set at 0.3. The solid and dotted lines in the figure indicate the prediction by the present model and the data of Sadatomi et al. (1982), respectively. Reasonably good agreement was obtained between them, if we take the ambiguity of the flow regime boundaries into account. The similar result was obtained for the 7 mm gap test section data (Sadatomi et al., 1982). Therefore, it can be concluded that the present model predicts the flow regime boundaries reasonably well for rectangular channels with a narrow gap as well as gap wider than 5 mm.

3.2. Steam–water flow at high pressures

The comparison of the newly developed flow-regime transition criteria with the data for high-pressure steam–water flow in a rectangular channel (Hosler, 1968) is presented in Fig. 9. Hosler used flowing quality x in order to account for subcooled boiling and for some of the effects

of heat flux, as mentioned by himself (Hosler, 1968). The Hosler maps in the flowing quality x-mass velocity G plane are transformed into those in the j_g–j_f plane. The superficial gas and liquid velocities can be calculated from the flowing quality and mass velocity by the following equations

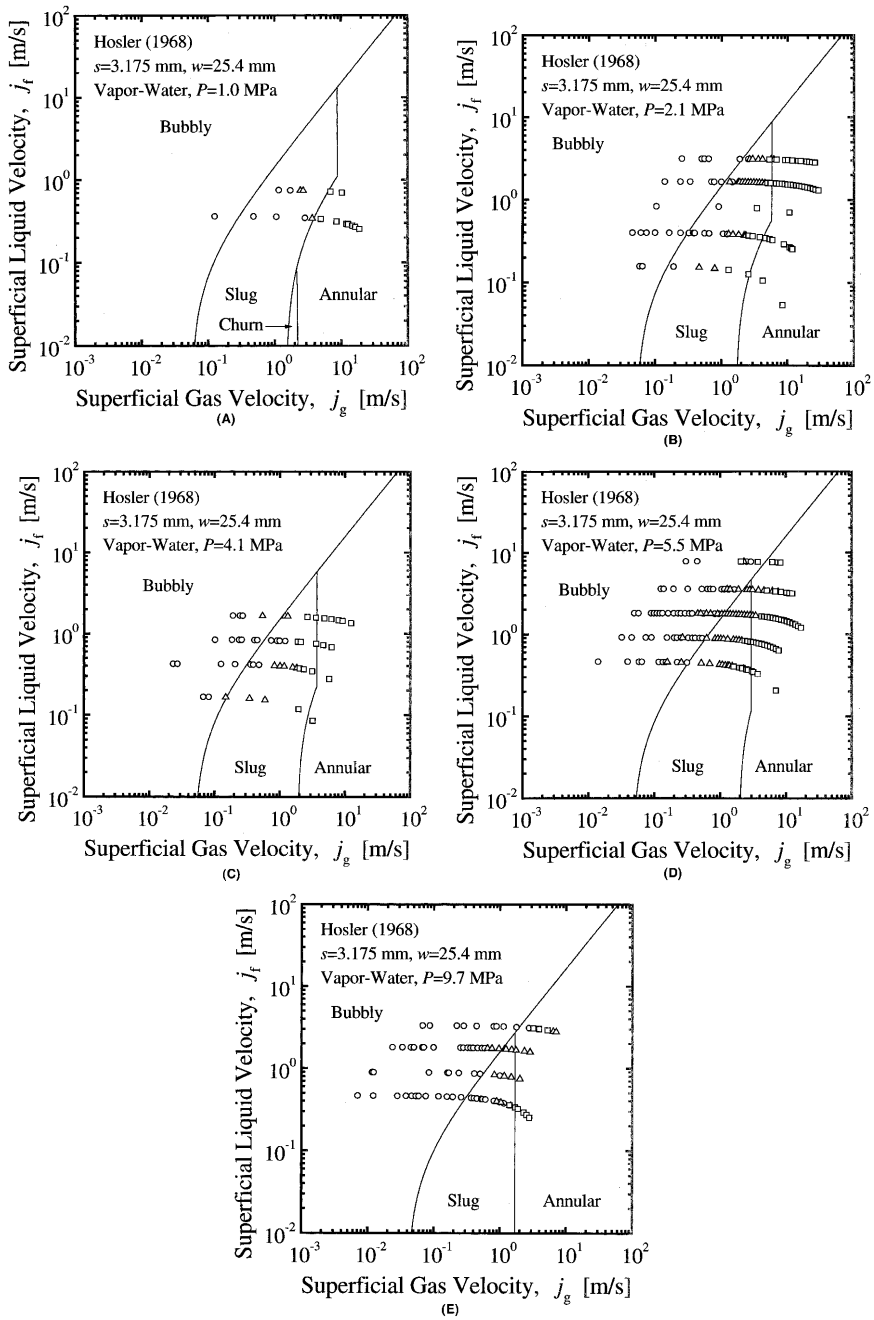

Fig. 9. Comparison for steam–water flow at relatively high pressure in a rectangular channel (data taken by Hosler (1968)). (a) $P = 1.0$ MPa, (b) $P = 2.1$ MPa, (c) $P = 4.1$ MPa, (d) $P = 5.5$ MPa, (e) $P = 9.7$ MPa.

$$G = \rho_g j_g + \rho_f j_f, \tag{32}$$

and

$$x = \frac{\rho_g j_g}{G}. \tag{33}$$

Fig. 9 shows that the general trends are predicted reasonably well by the present model of the flow-regime transition criteria, except that the agreement of the bubbly-to-slug flow transition is disappointing at 1.0 Mpa. However, Hosler himself limited the applicable range of pressure to 2–14 MPa for use of his data with reasonable confidence. The model of the flow-regime transition criteria indicate that the slug-to-annular flow transition occurs at lower gas velocities with increasing pressure, although the trend is less remarkable in the experimental data. As regards to boiling flow under low pressure, experimental observation indicates that boiling bubbles expand quickly over almost the entire boiling region, so that the flow regime is mostly churn flow or annular flow. In such a case, the comparison with this model has less meaning.

4. Summary and conclusions

Flow-regime transition criteria have been developed for the vertical upward flow in narrow rectangular channels. The basic concept of the modeling was the same as that of Mishima and Ishii model for round tubes. Newly developed criteria have been compared with the existing experimental data for air–water flows in narrow rectangular channels with the gaps from 0.3 to 17 mm as well as for steam–water flows in a rectangular channel with the gap of 3.175 mm at relatively high system pressures. The present criteria showed satisfactory agreements with those data. As far as the flow regime was classified by basic four patterns such as bubbly, slug, churn, and annular flows, the present flow-regime transition criteria could be applied over wide ranges of parameters as well as to boiling flow. However, in order to apply the present criteria to gaps narrower than 1 mm, a new model may be needed for the prediction of the distribution parameter for very narrow rectangular channels. Since very little data is available for a rectangular channel with the gap smaller than 1.0 mm, further experimental research should be encouraged for such an extremely narrow channel. A model for the flow regime transition criteria will be modified in accordance with new flow regimes to be observed in a rectangular channel with a micro gap.

Acknowledgements

The authors wish to acknowledge that the pioneering work of Professor Ishii (Purdue University, USA) has inspired the present research. The authors would like to express their sincere appreciation to Professor Theofanous (University of California, Santa Barbara, USA), the editor of Nuclear Engineering and Design and the reviewers for their valuable comments. The authors would like to acknowledge also Ms. Tauna Lea Wilmarth Leonardi (Purdue University, USA) for her valuable discussions. One of the authors (T. Hibiki) wishes to thank Professor Hibiki (Tokyo Institute of Technology, Japan) for his support on the computational calculation. Part of this study was supported by grant-in-aid for scientific research from the Ministry of Education, Science, Sport and Culture (No. 12780385). This study was originally presented in the Third International Conference on Multiphase Flow in 1998.

Appendix A. Nomenclature

C_0	distribution parameter
C_f	shape factor
D_b	equivalent diameter of a sphere
D_h	equivalent diameter of a channel
f	wall friction factor
G	mass velocity
g	gravitational acceleration
h	distance from the nose of slug bubble
j	mixture volumetric flux

j_f superficial liquid velocity
j_g superficial gas velocity
L_b mean slug–bubble length at the transition from the slug-to-churn flow regime
l maximum possible distance between two bubbles
m exponent
$N_{\mu f}$ viscosity number defined by Eq. (30)
P pressure
R_b projected radius of a flat bubble
s channel gap
V_{gj} drift velocity
v_g gas velocity
v_{gs} gas velocity
v_{fsb} velocity of the liquid flowing down the wide side walls
v_r relative velocity between gas and liquid phases
w channel width
X parameter defined by Eq. (5) or Eq. (16)
X' parameter defined by Eq. (18)
x flowing quality
z axial position

Greek letters
α void fraction
α_m mean void fraction over the slug–bubble section at the transition
α_{sb} mean void fraction over the slug–bubble section
γ coefficient
γ' coefficient
δ liquid layer thickness in the span-wise direction
δ_s liquid layer thickness in the span-wise direction
δ_w liquid layer thickness in the gap-wise direction
$\Delta\rho$ density difference between phases
μ viscosity
ν kinetic viscosity
ξ parameter defined by $\log(w/s)$
ρ density
σ surface tension
τ_i interfacial shear stress
τ_{wf} wall shear stress in the liquid film
χ parameter defined by Eq. (9)

Subscripts
f liquid phase
g gas phase
i interface
l laminar flow
l0 laminar flow in a round tube
t turbulent flow
t0 turbulent flow in a round tube

References

Ali, M., Kawaji, M., Sadatomi, M., 1993. Adiabatic two-phase flow in narrow channels between two flat plates. Can. J. Chem. Eng. 71, 657–666.
Bonjour, J., Lallemand, M., 1998. Flow patterns during boiling in a narrow space between two vertical surfaces. Int. J. Multiphase Flow 24, 947–960.
Griffith, P., 1963. The prediction of low quality boiling void. ASME Preprint 63-HT-20.
Hosler, E.R., 1968. Flow patterns in high pressure two-phase (steam–water) flow with heat addition. Chem. Eng. Prog. Symp. 64, 54–66.
Ishii, M., 1977. One-dimensional drift-flux model and constitutive equations for relative motion between phases in various two-phase flow regimes. ANL report ANL-77-47.
Itatani, M., 1966. Hydrodynamics (Suirikigaku in Japanese). Asakura, Tokyo, Japan, p. 134.
Lowry, B., Kawaji, M., 1988. Adiabatic vertical two-phase flow in narrow flow channels. AIChE Symp. Series 84, 133–139.
Mishima, K., Hibiki, T., 1996. Some characteristics of air–water two-phase flow in small diameter vertical tubes. Int. J. Multiphase Flow 22, 703–712.
Mishima, K., Hibiki, T., Nishihara, H., 1993. Some characteristics of gas–liquid flow in narrow rectangular ducts. Int. J. Multiphase Flow 19, 115–124.
Mishima, K., Ishii, M., 1984. Flow regime transition criteria for upward two-phase flow in vertical tubes. Int. J. Heat Mass Transfer 27, 723–737.
Moriyama, K., Inoue, A., Ohira, H., 1992a. The thermohydraulic characteristics of two-phase flow in extremely narrow channels (the frictional pressure drop and heat transfer of boiling two-phase flow, analytical model). Trans. JSME 58, 393–400.
Moriyama, K., Inoue, A., Ohira, H., 1992b. The thermohy-

draulic characteristics of two-phase flow in extremely narrow channels (the frictional pressure drop and void fraction of adiabatic two-component two-phase flow). Trans. JSME 58, 401–407.

Sadatomi, M., Sato, Y., Saruwatari, S., 1982. Two-phase flow in vertical noncircular channels. Int. J. Multiphase Flow 8, 641–655.

Taitel, Y., Bornea, D., Dukler, A.E., 1980. Modelling flow pattern transitions for steady upward gas–liquid flow in vertical tubes. AIChE J. 26, 345–354.

Wallis, G.B., 1969. One Dimensional Two-Phase Flow. McGraw-Hill, New York, pp. 318–322.

Wilmarth, T., Ishii, M., 1994. Two-phase flow regimes in narrow rectangular vertical and horizontal channels. Int. J. Heat Mass Transfer 37, 1749–1758.

Wilmarth, T., Ishii, M., 1997. Interfacial area concentration and void fraction of two-phase flow in narrow rectangular vertical channels. J. Fluids Eng. 19, 916–922.

Xu, J., 1999. Experimental study on gas–liquid two-phase flow regimes in rectangular channels with mini gaps. Int. J. Heat Fluid Flow 20, 422–428.

Xu, J.L., Cheng, P., Zhao, T.S., 1999. Gas–liquid two-phase flow regimes in rectangular channels with mini/micro gaps. Int. J. Multiphase Flow 25, 411–432.